

A ^1H Nuclear Magnetic Resonance Study of the Opioid Peptide Dynorphin-(1-13) in Aqueous Solution

Ning Zhou

Department of Biochemistry, University of Wisconsin-Madison, Madison, Wisconsin 53706, U.S.A.

William A. Gibbons*

Department of Pharmaceutical Chemistry, School of Pharmacy, University of London, 29/39 Brunswick Square, London, WC1N 1AX

A ^1H n.m.r. study of the conformation of the opioid peptide dynorphin-(1-13) was performed in aqueous solution using one-dimensional (1D) and two-dimensional (2D) n.m.r. techniques. Chemical shifts, scalar $^3J_{\alpha\beta}$ values, amide proton-deuteron exchange rates, temperature coefficients of chemical shifts, and spin-label perturbation of amide proton relaxation rates formed a self-consistent picture of a polypeptide chain possessing no major preferred secondary conformations. 600 MHz 2D J -resolved spectroscopy was used to analyse the coupling patterns for the constituent amino acid residues. Side-chain rotamer analysis based upon $^3J_{\alpha\beta}$ coupling constants for five of the residues indicated no significantly large populations of any χ_1 rotamers.

Dynorphin, a potent opioid peptide, has been isolated from both the porcine pituitary¹ and the porcine duodenum.² Its amino sequence, Tyr¹-Gly²-Gly³-Phe⁴-Leu⁵-Arg⁶-Arg⁷-Ile⁸-Arg⁹-Pro¹⁰-Lys¹¹-Leu¹²-Lys¹³-Trp¹⁴-Asp¹⁵-Asn¹⁶-Gln¹⁷,² contains the [Leu⁵]-enkephalin sequence at the N-terminal. The N-terminal 13-peptide of dynorphin, dynorphin-(1-13), displayed the same potency as the intact 17-peptide in the bioassay based on inhibition of electrically evoked contractions of the guinea pig ileum (GPI).^{1,2} This implies that the sequence of dynorphin-(1-13) is important in receptor binding and in biological functioning. Synthetic dynorphin-(1-13) was used for a 1D and 2D ^1H n.m.r. study of its conformation in aqueous solution.

Experimental

The dynorphin-(1-13) sample was kindly provided by Dr. M. W. Moon, Upjohn Company, Kalamazoo, Michigan and demonstrated to be pure by reverse-phase h.p.l.c., t.l.c., and amino acid analysis.

The two-dimensional spin-echo correlated and two-dimensional J -resolved spectra (Figures 1 and 2), and the proton decoupling experiments (Figure 5), were run at the NMR Facility for Biomedical Studies on the Carnegie-Mellon Institute 600 MHz spectrometer. The sample concentration for two-dimensional experiments was 10mM in 100% D_2O (Aldrich), pD 3.9. The pulse sequence used for the spin-echo correlated spectrum was $(T-P_{90}-0.5t_1-P_{90}-0.5t_1\text{-acquisition } t_2)_n$ with t_1 incremented equally for successive experiments; 112 scans were accumulated for each experiment and the resolution in both dimensions was 5.14 Hz/point. The pulse sequence $(T-P_{90}-0.5t_1-P_{180}-0.5t_1\text{-acquisition } t_2)_n$ was used for the J -resolved spectrum with t_1 incremented equally for successive experiments and 256 scans were collected for each experiment. The resolution in the F1 dimension (coupling constant) was 0.305 Hz/point and in the F2 dimension (chemical shift) it was 2.441 Hz/point. The sweep width in the F1 dimension was 50 Hz, thus the fold back of weak peaks from strong coupling patterns of side-chain aliphatic protons was possible. The residual water peak was decoupled during the two-dimensional experiments to reduce its intensity. In processing the data, one zero filling was used in both dimensions and sine bell function multiplication was used before Fourier transformation to achieve desired resolution enhancement. The magnitude spectrum was used for the J -resolved spectroscopy representations.

The underwater decoupling experiments for Gly α protons were performed in 100% H_2O solution using correlation spectroscopy,³ with field locking on the water proton signal.

The temperature dependence and spin-label studies were performed on a Bruker 270 MHz spectrometer equipped with a Nicolet 1180 computer. A 4.62mM-dynorphin sample in 100% D_2O was used for non-exchangeable proton studies. For amide proton chemical-shift studies, a 6.25mM-dynorphin sample in 10% D_2O -90% H_2O (pH 3.9) was used.

In the spin-label experiments, the spin-lattice relaxation times, T_1 , were measured using the inversion-recovery sequence.⁴ A stock solution of 70mM-2,2,6,6-tetramethyl-4-hydroxypiperidin-1-oxyl (TEMPOL) in pure D_2O was made, and small amounts of stock solution were added to the sample to give different TEMPOL concentrations.

Results and Discussion

Assignments.—The assignments of the aromatic-ring protons, α protons, and side-chain protons were achieved using 2D chemical-shift-correlated spectroscopy (Figure 1) and 2D J -resolved spectroscopy (Figure 2), and confirmed where necessary by 1D double-resonance difference spectroscopy. The chemical shifts and coupling constants are listed in Table 1. From the projection representation of the J -resolved spectrum (Figure 3), the eleven α proton multiplets (except those for the two Gly residues) in the range δ 4.0–4.7 were all resolved giving the chemical shifts of these protons. Their splitting patterns were seen in cross-sections taken at these chemical-shift positions (Figure 4a). The α - β coupling connectivities for these amino acid residues were identified from the spin-echo correlated experiments and are shown in the expanded contour plot (Figure 5). The α protons of the two Gly residues showed strong coupling patterns (see below).

Tyr¹ and Phe⁴. These two residues were distinguished from others because of the downfield β proton resonances⁵ (Table 1) (δ 3.15, 3.15 for Tyr¹ and δ 3.11, 3.02 for Phe⁴, compared with other β proton resonances in the range δ 1.52–1.85). One of these two α protons was found at an unusually high field position (δ 4.25) relative to the random coil peptide α proton chemical-shift values for Tyr and Phe residues (δ 4.60 and 4.66, respectively⁵). This was attributed to the effect of the N-terminal on the Tyr α proton and thus distinction was made between Tyr and Phe α protons. Owing to the degeneracy of the two β protons of Tyr¹, the Tyr¹ α - β spin system was a simple

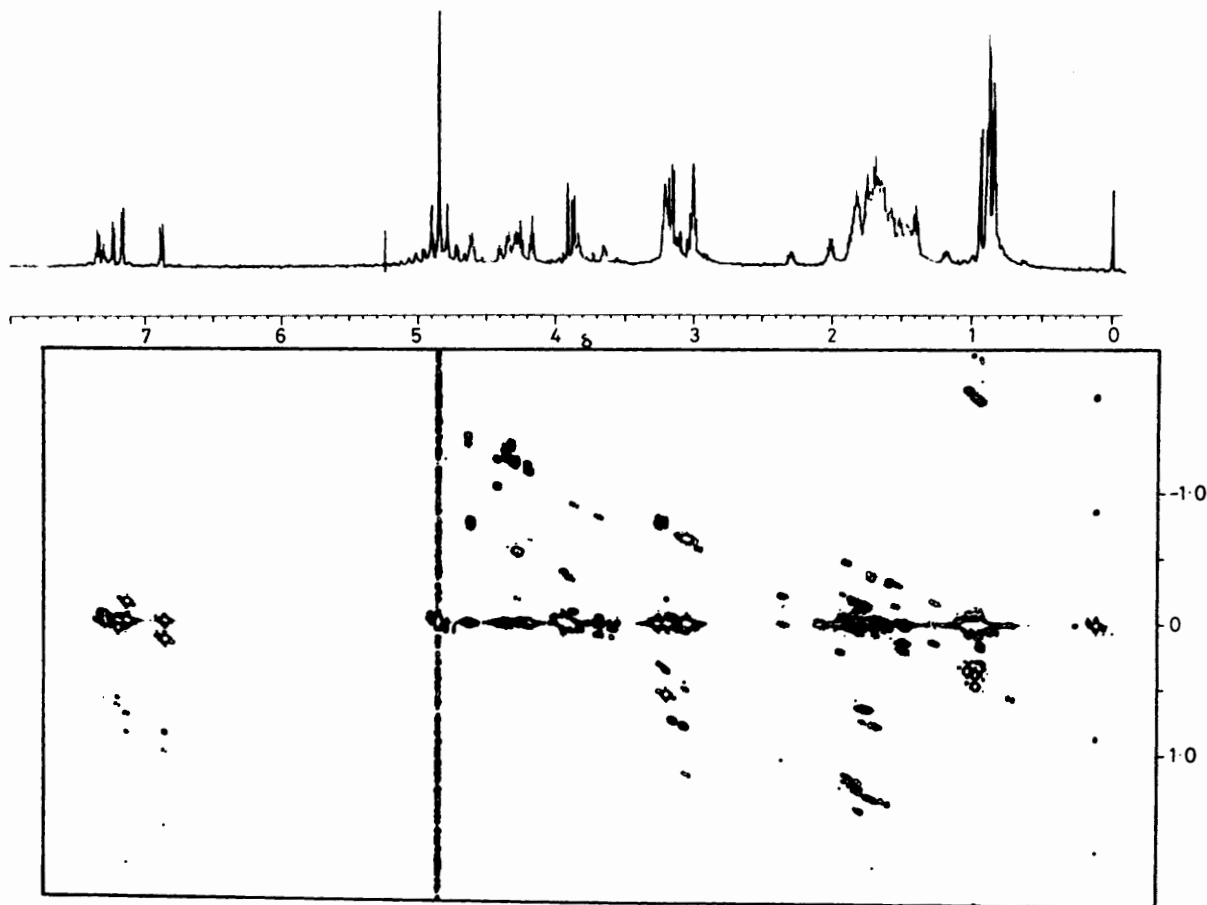


Figure 1. A 600 MHz ^1H n.m.r. spectrum of dynorphin-(1-13) in D_2O (above) and a contour plot of a 600 MHz 2D spin-echo correlated spectrum (lower) of the same sample

Table 1. Chemical shifts and coupling constants

Residue	Chemical shift δ^a							J/Hz		
	δ_{NH}	δ_{H_α}	$\delta_{\text{H}_{\beta\alpha}}$	$\delta_{\text{H}_{\beta\beta}}$	Other			$J_{\text{NH}-\alpha}$	$J_{\alpha-\beta_\alpha}$	$J_{\alpha-\beta_\beta}$
Tyr ¹		4.25	3.15	3.15	H_δ 7.17	H_ϵ 6.88				
Gly ²	8.57	3.92	3.90					5.73	-16.79	
Gly ³	7.93	3.88	3.85	($\delta_{\text{H}_{\beta\alpha}}$)				6.03	-16.79	
Phe ⁴		4.60	3.11	3.02	H_δ 7.24	H_ϵ 7.36	H_ζ 7.31			
Ile ⁵		4.16	1.83		H_{γ_α} 1.46	H_{γ_β} 1.92	$\text{H}_{\gamma_{\text{CH}_3}}$ 0.88	$\text{H}_{\delta_{\text{CH}_3}}$ 0.84		
Pro ¹⁰		4.40	2.30	1.88	H_γ 2.01	H_{δ_α} 3.83	H_{δ_β} 3.65			
Lys ¹¹		4.18	1.75	1.72	H_γ 1.40	H_δ 1.70	H_ϵ 3.01			
Lys ¹³		4.62	1.73	1.67	H_γ 1.40	H_δ 1.70	H_ϵ 3.02			
Leu ^{5*}		4.35	1.66	1.62	H_γ 1.65	H_{δ_α} 0.94	H_{δ_β} 0.88			
Leu ^{12*}		4.33	1.56	1.52	H_γ 1.52	H_{δ_α} 0.90	H_{δ_β} 0.85			
Arg ^{6†}		4.30	1.85	1.80	H_γ 1.72	H_δ 3.22				
Arg ^{7†}		4.29	1.80	1.74	H_γ 1.63	H_δ 3.22				
Arg ^{9†}		4.27	1.76	1.73	H_γ 1.60	H_δ 3.16				

^a Chemical shifts were reported relative to internal standard 3-(trimethylsilyl)propanesulphonic acid sodium (DSS) salt.

*,[†] Groups of residues which were not unambiguously assigned.

AX₂ system. The cross-section representation for Tyr¹ α and β protons are included in Figures 4a and b, respectively.

Gly² and Gly³. The amide protons of these two residues are the only two triplets in the spectrum taken in 100% H₂O

solution (Figure 6). Amide α couplings for the two Gly residues were detected by decoupling experiments under the same condition (Figure 6). The chemical-shift change of the downfield amide proton during pH titrations was determined as 0.14

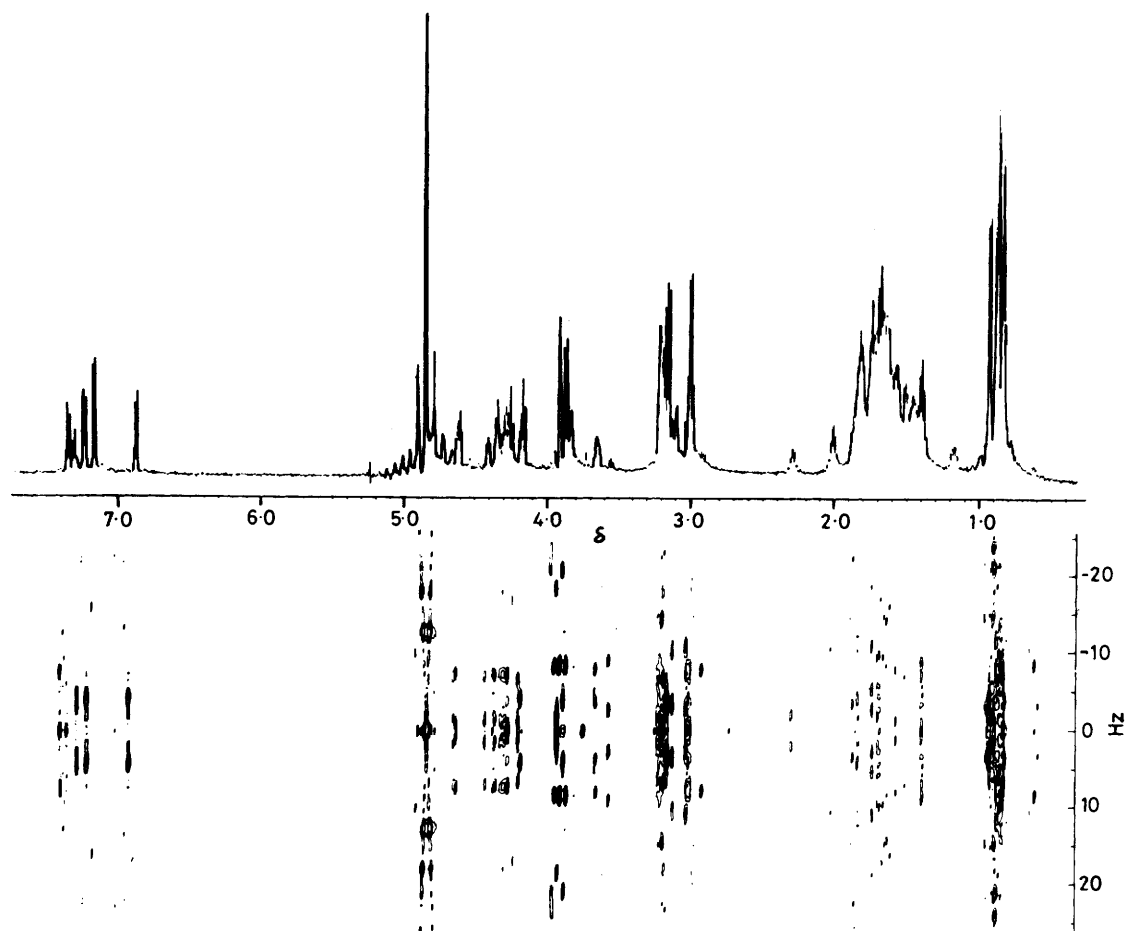


Figure 2. A 600 MHz ^1H n.m.r. spectrum of dynorphin-(1-13) in D_2O (above) and a contour plot of a 600 MHz 2D J -resolved spectrum (lower) of the same sample

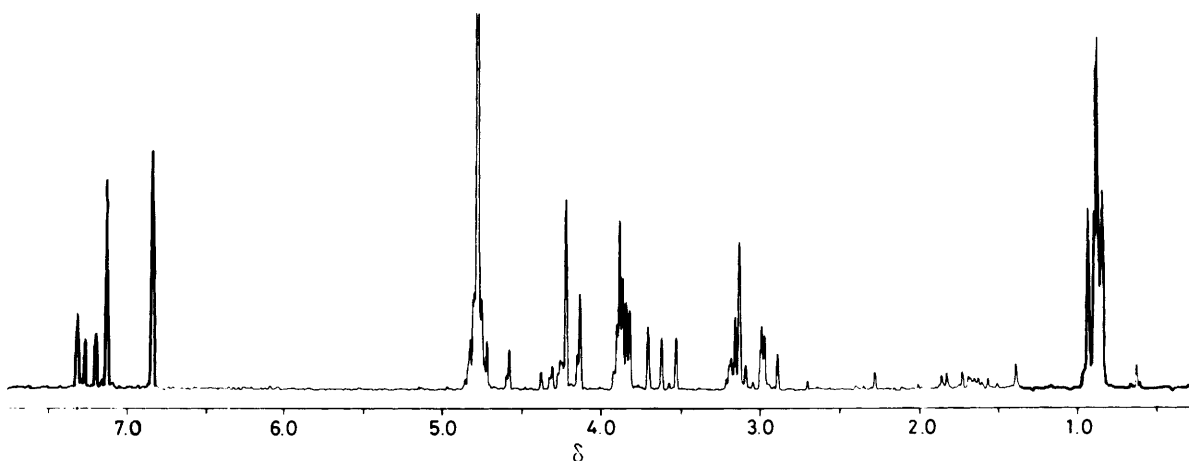


Figure 3. Projection along the J axis onto the chemical-shift axis of the 600 MHz 2D J -resolved spectrum (Figure 2), that is, a proton homonuclear broad-band decoupled spectrum of dynorphin-(1-13)

p.p.m. per pH unit and the other was 0.10 p.p.m. per pH unit in the range pH 2–5. The downfield one was therefore assigned to Gly^2 , since it would experience a larger pH shift upon the N-terminal titration.

The α protons of both the Gly^2 and Gly^3 residues formed a strongly coupled AB spin systems. The two peripheral doublets

of Gly^2 were identified at δ 3.93 and 3.89, and of Gly^3 at δ 3.89 and 3.85; extra central multiplets appear at δ 3.91 for Gly^2 and at δ 3.87 for Gly^3 (Figure 4b). The chemical shifts and coupling constants were obtained by computer-iterated fit of the 1D experimental spectra.

Several amino acid residues possess unique spin-spin sys-

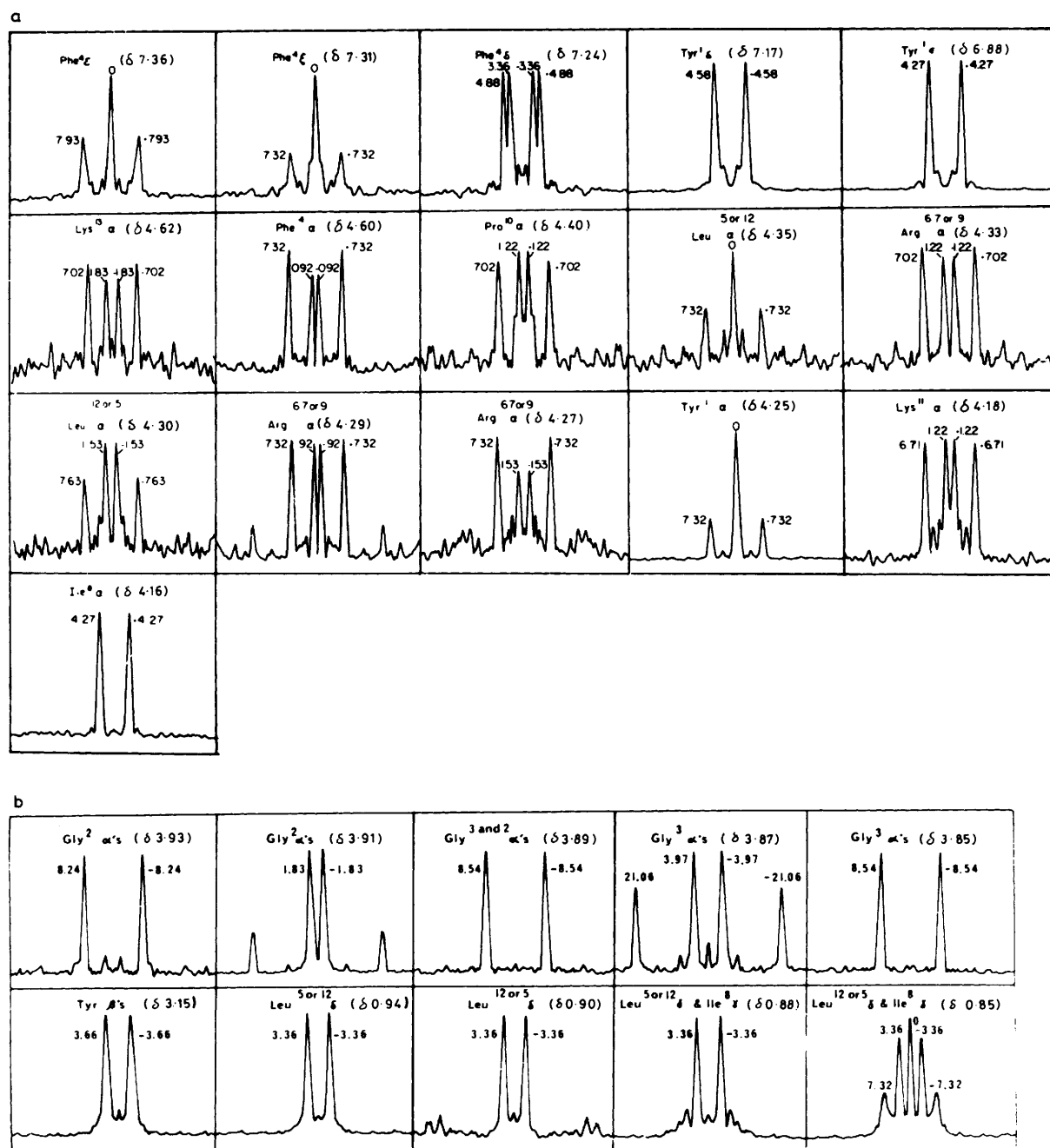


Figure 4. (a and b) Selected cross-section representations of some multiplets in the 600 MHz 2D J -resolved spectrum (Figure 2) of dynorphin. The label for each section shows the chemical-shift position where the cross-section was taken and the assignment at this position. Multiplets were labelled by Hz from the middle

tems that were readily identified from two-dimensional spin-echo spectra. The J -connectivities for the Ile⁸ and Pro¹⁰ residues were marked on a contour plot of a two-dimensional spin-echo correlated spectrum in Figure 5; for the Ile⁸ residue, all the J -connectivities showed up clearly. The whole spin-spin system of the Pro¹⁰ residue was completely identified except for the β_a - γ and β_w - γ connectivities which appeared on one side only. These assignments and analyses were further supported by the multiplet structure in the two dimensional J -resolved spectrum (a doublet at δ 4.16 for Ile α proton and a doublet of doublets at δ 4.60 for Pro α proton) (see Figures 4a and 2).

Lys¹¹ and Lys¹³. The two Lys ϵ proton signals were identified

in the chemical-shift range δ 2.85–3.10. There were no other signals in this range except the half of the Phe β proton AB pattern in the ABX spin system of the Phe residue. The Phe β signals were clearly separated from the Lys ϵ signals in the two-dimensional spin-echo correlated spectrum (Figure 5). Lys ϵ - δ , δ - γ , and γ - β connectivities were then identified sequentially, and from Lys β , two Lys α signals were identified. One Lys α (δ 4.62) (Table 1) was significantly downfield shifted compared with random coil data of Bundi *et al.*,⁵ and this was tentatively assigned to Lys¹³. To avoid overcrowding, these J -connectivities were not marked on the two dimensional contour plot (Figure 5).

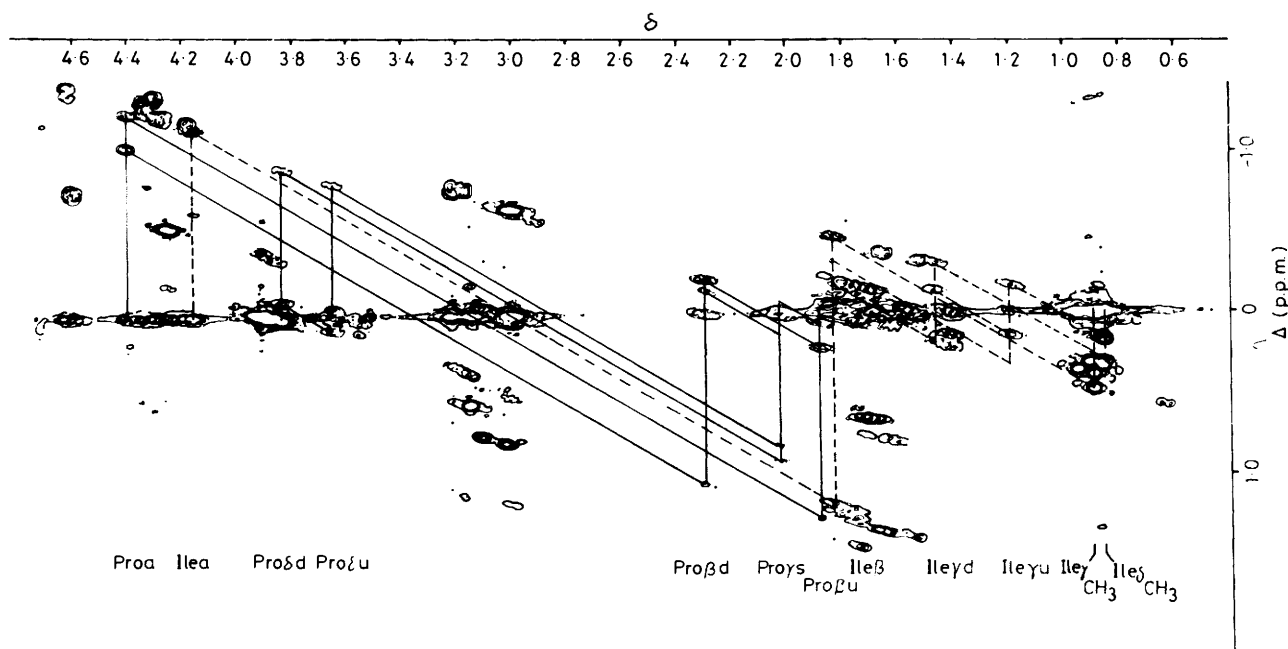


Figure 5. Upfield region expansion of the 600 MHz spin-echo correlated spectrum in Figure 1. The J coupling connectivities for amino acid residue Pro and Ile were marked

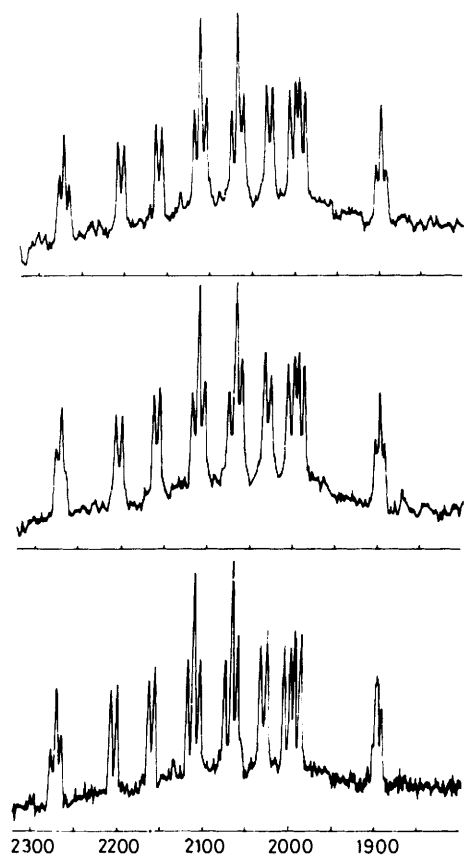


Figure 6. Amide proton region of 600 MHz proton spectra of dynorphin-(1-13) in H_2O . The top trace, with the decoupler located at 30 Hz upfield from Gly^2 α protons (off-resonance). The middle trace and the lower trace are with the decoupler at Gly^3 α and Gly^2 α protons, respectively. The axis is labelled downfield from the H_2O signal in Hz

Leu^5 and Leu^{12} . Although the δ_{CH_3} - γ connectivities for the two Leu residues were clear (Figure 5), the γ - β connectivities were ambiguous and therefore the α - β connectivities for the two individual Leu residues were not identified. The multiplet structure for all 13 α protons were resolved in the 2D J -resolved spectrum, but sequence assignments of the two Leu residues and the three Arg residues (see below) was not achieved. The methyl proton resonances of Ile and Leu residues showed weak coupling patterns; their cross-section representations of the J -resolved spectroscopy were included in Figure 4b.

Arg^6 , Arg^7 , and Arg^9 . The δ - γ connectivities for three Arg residues were identified (Figure 5), but other connectivities were not unambiguously assigned due to both low intensities of cross-peaks (high multiplicity) and extensive overlap. The 2D J -resolved spectra of amino acid side-chain aliphatic protons usually show complex strong coupling patterns (Figure 2) and hence are not helpful in assignments.

There are several other notable features of the proton n.m.r. spectrum of dynorphin-(1-13). In the aromatic region, the δ and ϵ protons of the Tyr residue and of the Phe residue are both degenerate, indicating that the aromatic rings of both Phe and Tyr residues exhibit fast X_2 rotation in solution. The coupling constants $^3J_{NH-H}$ (see Table 1) are in the range 5.7–7.5 Hz, which is not very different from the reported values for random coil peptides.⁵

Figure 7 shows a comparison of the experimental and computer-simulated spectra for the aromatic ring protons and for eight α protons (α protons of residues Lys^{13} , Phe^4 , Pro^{10} , Tyr^1 , Lys^{11} , Ile^8 , Gly^2 , and Gly^3). For the two Leu and three Arg residues, coupling constants $^3J_{H-H}$ were not obtained and simulation was not attempted. The spectral analysis in this region was confirmed by the agreement between simulated and experimental spectra.

Side-chain Rotamers.—The side-chain rotamer analysis based upon $^3J_{H-H}$ coupling constants for some amino acid residues is in Table 2. It was assumed that the side-chain orientations were confined to those of the classically allowed

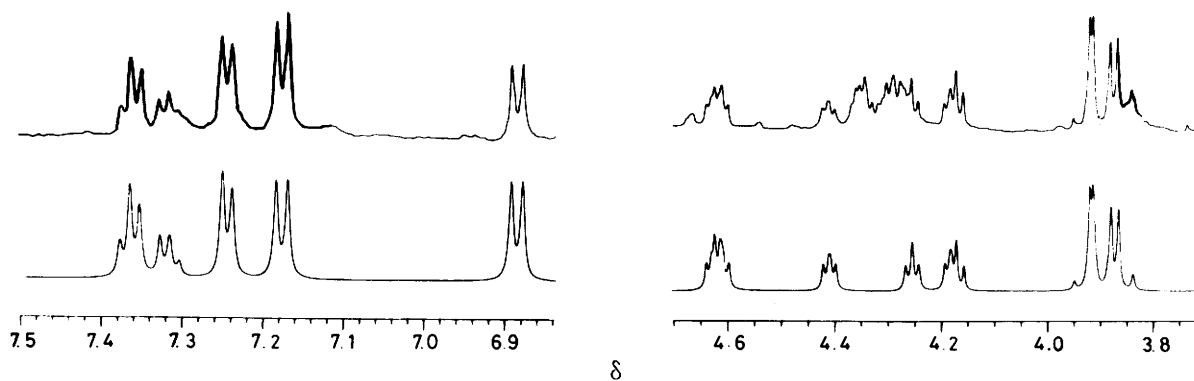


Figure 7. A comparison of 600 MHz experimental proton spectrum of dynorphin (upper traces) with the computer-simulated spectrum (lower traces). Those on the left represent the whole aromatic-ring-proton region, while those at the right represent the α region. The simulation in the α region only includes α protons for 8 out of 13 amino acid residues (see text). The small peak at δ ca. 4.67 is the spinning side-band of the HDO peak at δ 4.78. Note also that one Pro δ (δ 3.83) signal was under Gly³ α signals in the experimental spectrum but was not included in the simulated spectrum

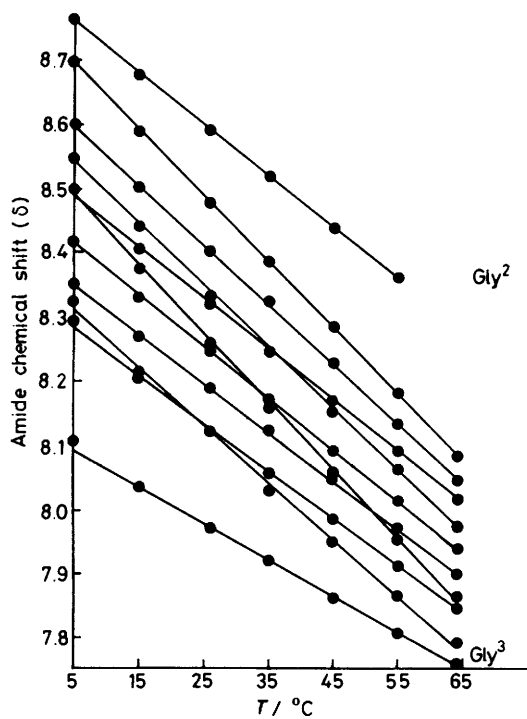


Figure 8. Dynorphin-(1-13) amide proton chemical shifts versus experimental temperatures

staggered rotamers and that $^3J_{trans} = 13.59$ and $^3J_{gauche} = 2.60$ Hz.⁶

The side-chain rotamer analysis performed for the Tyr¹, Phe⁴, Ile⁸, Lys¹¹, and Lys¹³ residues showed that at least two of the classically allowed rotamers are significantly populated and that there is not a preferred orientation for these side-chains in solution; the most highly populated χ_1 state of these residues was $\chi_1 = 59\%$ for Lys¹³ (Table 2).

Temperature Dependence.—The temperature dependences of amide proton chemical shifts are shown in Figure 8. In the temperature range studied, the chemical-shift changes with temperature for all the protons were linear. The temperature coefficients $\Delta\delta/\Delta T$ for Gly³ amide proton was -5.71 p.p.b./°C, and varied from -7.40 to -10.70 p.p.b./°C for the other ten amide protons. The value for Gly³ was considered large

Table 2. Side-chain rotamer populations of dynorphin-(1-13)†

Residue	Population (%)		
	$\chi_1 = 180^\circ$	$\chi_1 = -60^\circ$	$\chi_1 = 60^\circ$
Tyr ¹	43	43	14
Phe ⁴	36	57	7
Lys ¹¹	22	46	32
Lys ¹³	27	59	14
Ile ⁸	*	57	*

* These two rotamers add up to 43%. † The populations for the $\chi_1 = 180^\circ$ and $\chi_1 = -60^\circ$ rotamers could be reversed for Tyr, Phe, and Lys due to the lack of assignment of *pro-R* and *pro-S* β protons.

Table 3. Paramagnetic spin label effects on the spin-lattice relaxation rate R_1 ,* of some dynorphin protons†

Proton	[TEMPOL]/mM				$S_{1p}^\ddagger/$ l mol ⁻¹ s ⁻¹
	0	0.5	1.5	2.5	
Tyr ϵ	0.52	0.90	1.17	1.61	430
Tyr δ	0.97	1.30	1.55	1.98	400
Phe ring	1.07	1.34	1.62	2.07	400
Phe α	1.48	1.80	2.17	2.59	450
Pro α	1.05	1.48	1.85	2.50	555
Ile α	1.30	1.71	2.09	2.50	490
Glu ² α	2.65	2.86	3.29	3.63	400
Gly ³ α	2.93	3.10	3.63	3.93	405

* Spin-lattice relaxation rate R_1 ($R_1 = 1/T_1$) values are listed in units of s⁻¹. † The dynorphin sample concentration was 4.62mM in D₂O. ‡ S_{1p}^\ddagger indicates the increment of proton R_1 value per mole of added paramagnetic compound TEMPO.

compared with temperature coefficients for typical solvent-shielded or hydrogen-bonded amide protons in aqueous solution, ≤ -3.0 p.p.b./°C.⁷ The temperature dependences of the non-labile protons were linear and very small (0–0.63 p.p.b./°C). There was no indication of significant amide proton involvement in intramolecular hydrogen-bond formation, and no evidence for co-operative conformation changes within this temperature range.

Spin-label Study.—Spin-lattice relaxation rates R_1 for some of the protons were measured in the absence and presence of paramagnetic nitroxide 2,2,6,6-tetramethyl-4-hydroxypiperidin-1-oxyl (TEMPOL); the results are listed in Table 3. The

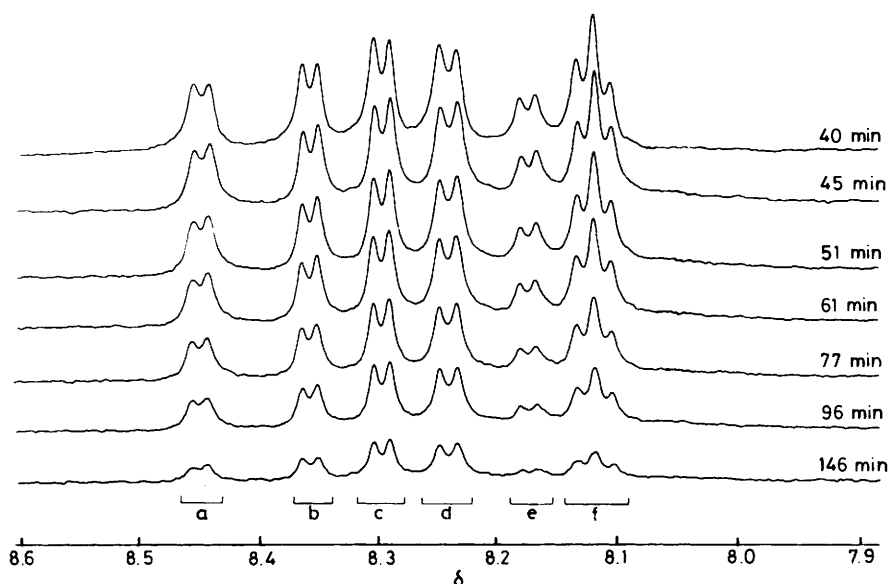


Figure 9. 500 MHz Amide proton spectra of dynorphin-(1-13) at different times after the sample was dissolved in D_2O . The times are indicated at the right side of the spectra. The areas under c, d, and f were for two protons each but were counted together to get an averaged apparent first-order exchange rate (see Table 4)

Table 4. Amide H-D exchange rates of dynorphin-(1-13)

Peak area *	a	b	c	d	e	f	Gly ²	Gly ³
Apparent first-order exchange rate $10^2 k/\text{min}^{-1}$	1.37	1.66	1.16	1.38	2.18	1.70	>25	11

* Peak areas were those marked on Figure 9. Areas a, b, and e each represent one amide proton; areas c, d, and f each represent two amide protons. In a separate experiment, the exchange rate for Gly³ was determined and the rate of Gly² was approximated.

relationship of enhancement of relaxation rates R_1/s^{-1} versus nitroxide concentration were linear for all the protons studied and the increment of R_1 per mole of TEMPO added, $S_{1p}/l \text{ mol}^{-1} s^{-1}$,⁸ was in the range 400–550 for all aromatic and α protons. The large S_{1p} values suggested general solvent exposure of these protons,⁸ consistent with the interpretation of the temperature dependence of their chemical shifts.

Amide H-D Exchange.—The H-D exchange experiments for amide protons were carried out using freshly dissolved dynorphin-(1-13) D_2O solution (pH 2.75) at 4 °C, and the decrease in amide peak areas followed as a function of time. Due to spectral overlap, exchange rates for several pairs of amide protons were measured together (Figure 9). The resulting apparent first-order exchange rates are listed in Table 4. The overlapping amide proton peaks exhibited similar exchange rates (Figure 9). The Gly² amide proton exchanges with a rate faster than $2.5 \times 10^{-1} \text{ min}^{-1}$ and the Gly³ amide proton exchange rate was determined to be $1.1 \times 10^{-1} \text{ min}^{-1}$; all other amide protons had exchange rates in the range 1.2×10^{-2} – $2.2 \times 10^{-2} \text{ min}^{-1}$ under these conditions. These exchange rates are larger than the predicted rates ($2.4 \times 10^{-1} \text{ min}^{-1}$ for Gly², $2.3 \times 10^{-2} \text{ min}^{-1}$ for Gly³, and 0.68 – $0.93 \times 10^{-2} \text{ min}^{-1}$ for all other amide protons) from the data of Molday *et al.*⁹ and are comparable with the amide H-D exchange rates of oxidized random coil RNAase, 10^{-1} – 10^{-3} min^{-1} .¹⁰ Therefore the amide

H-D exchange behaviour suggested a non-structured form for dynorphin with all amide protons well exposed to solvent.

The results from ¹H n.m.r. spectroscopy are consistent with a reported c.d. study of dynorphin-(1-13) in aqueous solution¹¹ in which the spectrum exhibited little, if any, ordered structure for dynorphin-(1-13). We measured the c.d. spectrum of dynorphin-(1-13) in a H_2O -MeOH solvent system. Addition of up to 55% MeOH did not cause a significant change in the spectrum.

The intramolecular distance between the Tyr¹ side-chain and the Trp⁴ side-chain was found to be at least 15 Å in a fluorescence study of the [Trp⁴] dynorphin-(1-13) analogue.¹² This too was consistent with a random conformation of the molecule.

Thus, under the experimental conditions, dynorphin-(1-13) appears to exist mainly in the non-ordered form.

Acknowledgements

This research was partially supported by the School of Pharmacy, London University, and by the College of Agriculture and Life Sciences and the Graduate School of the University of Wisconsin-Madison and by federal grants from the NIH and the NSF. N. Z. was a Steenbock predoctoral fellow of the Biochemistry Department, University of Wisconsin-Madison. We thank the NMR Facility for Biomedical Research at Carnegie-Mellon Institute. The calculation of predicted amide proton H-D exchange rates was done by Dr. L. Buffington.

References

- 1 A. Goldstein, S. Tachibana, L. I. Lowney, M. Hunkapiller, and L. Hood, *Proc. Natl. Acad. Sci. U.S.A.*, 1979, **76**, 6666.
- 2 S. Tachibana, K. Araki, S. Ohya, and S. Yoshida, *Nature (London)*, 1982, **295**, 339.
- 3 J. Dadok and R. F. Sprecher, *J. Magn. Reson.*, 1974, **13**, 243.
- 4 H. Y. Carr and E. M. Purcell, *Phys. Rev.*, 1954, **94**, 630.
- 5 A. Bundi and K. Wuthrich, *Biopolymers*, 1979, **18**, 285.
- 6 K. G. R. Pachler, *Spectrochim. Acta*, 1964, **20**, 581.

- 7 A. H. Gordon, A. J. P. Martin, and R. L. M. Synge, *Biochem. J.*, 1943, **37**, 86.
- 8 N. Nicolai, G. Valensin, C. Rossi, and W. A. Gibbons, *J. Am. Chem. Soc.*, 1982, **104**, 1534.
- 9 R. S. Molday, S. W. Englander, and K. G. Kallen, *Biochemistry*, 1972, **11**, 150.
- 10 C. K. Woodward and A. Rosenberg, *Proc. Natl. Acad. Sci. U.S.A.*, 1970, **66**, 1067.
- 11 R. Maroun and W. L. Mattice, *Biochem. Biophys. Res. Commun.*, 1981, **103**, 442.
- 12 P. W. Schiller, *Int. J. Peptide Protein Res.*, 1983, **21**, 307.

Received 11th July 1984; Paper 4/1203